M. KUPKOVÁ*, M. HRUBOVČÁKOVÁ*, A. ZELEŇÁK*, M. SUŁOWSKI**,♯, A. CIAŚ**, R. ORIŇÁKOVÁ***,
A. MOROVSKÁ TUROŇOVÁ***, K. ŽÁKOVÁ***, M. KUPKA****

DIMENSIONAL CHANGES, MICROSTRUCTURE, MICROHARDNESS DISTRIBUTIONS AND CORROSION PROPERTIES OF IRON AND IRON-MANGANESE SINTERED MATERIALS

ZMIANY WYMIAROWE, MIKROSTRUKTURA, ROZKŁAD MIKROTWARDOŚCI I WŁASNOŚCI KOROZYJNE SPIEKANYCH MATERIAŁÓW ŻELAZO ORAZ ŻELAZO-MANGAN

Iron samples and Fe-Mn alloys with Mn content of 25 wt.% and 30 wt.% were prepared by blending, compressing and sintering with the aim to study their dimensional changes, microstructure, microhardness distribution and primarily the electrochemical corrosion behaviour in a simulated body environment.

The light microscopy (LM), scanning electron microscopy (SEM), energy-dispersive X-ray spectroscopy (EDX) and micro-hardness measurements revealed a microheterogeneous multiphase structure of sintered Fe-Mn samples. The potentiodynamic tests have demonstrated that the corrosion rates of such Fe-Mn alloys immersed in Hank's solution were higher than those for a pure iron, and also higher than the rates reported for homogeneous Fe-Mn alloys.

Keywords: powder metallurgy, iron, manganese, corrosion behaviour, dimensional changes, microhardness

Próbki żelazne oraz stopy Fe-Mn, zawierające 25 i 30% mas. Mn, przeznaczone na biomateriały, zostały przygotowane na drodze mielenia, prasowania oraz spiekania w celu zbadania ich zmian wymiarowych, mikrostruktury, rozkładu mikrotwardości oraz odporności korozyjnej w skumulowanych w warunkach laboratoryjnych, panujących w ciele człowieka.

Badania z wykorzystaniem mikroskopii optycznej i skaningowej, wraz z EDX oraz pomiary mikrotwardości ujawniły mikroniejednorodność wielofazowej struktury spiekanych stopów Fe-Mn. Testy potentiometryczne wykazały, że współczynniki korozji spieków Fe-Mn były wyższe niż spieków wykonanych z czystego żelaza oraz z jednorodnych stopów Fe-Mn.

1. Introduction

A piece of metal can be easily formed into complexly-shaped objects possessing excellent mechanical properties. The metals are therefore used as implant materials in surgery for more than a century. During these years, a paradigm has been established that metals which are put into the human body should be highly corrosion-resistant to survive the harsh physiological environment.

Nevertheless, a quite general agreement has recently emerged that, for certain medical applications, the corrodibility can be a desirable material's property [1]. This is, for example, the case of corronary stents. The mechanical scaffolding effect provided by a stent is needed only temporarily for a period of 3-6 (6-12) months after stent implantation, during which arterial remodeling and healing occur. After this period, stent cannot provide any beneficial effect. Contrariwise, the permanent presence of implant in the arterial wall can trigger late complications such as restenosis, trombosis, etc. So, the short-term stent that provides a temporary support for the healing process and after some time decomposes in situ into non-toxic corrosion products which are readily excreted from the body would be clearly preferable over the currently-used permanent stents.

Metals belonging to the biogenic elements, such as Ca, Mg, Fe, Mn, Zn, ..., are naturally present in our body. Alloys which consist of these metals are therefore promising candidates for temporary stent materials.

Stents made of pure iron were implanted into various mammals [2-3]. There was no evidence for local toxicity due to corrosion products, no signs of iron overload or iron-related organ toxicity. However, iron stents remained mainly intact for up to a year after implantation. In addition, the mechanical properties of pure iron are modest and not particularly well suited for the use as stent material. To accelerate degradation and improve mechanical properties, Hermawan et al. [4-6] alloyed iron with manganese. The manganese has been chosen because it is less noble than iron, it is known as an austenite-forming element, and from a biological point of view, the excess of manganese is not reported to be toxic in cardiovascular system [6].

*   INSTITUTE OF MATERIALS RESEARCH, SLOVAK ACADEMY OF SCIENCES, WATSONOVA 47, SK-040 01 KOŠICE, SLOVAK REPUBLIC
**   AGH UNIVERSITY OF SCIENCE AND TECHNOLOGY, AL. A. MICKIEWICZ 30, 30-059 KRAKÓW, POLAND
*** DEPARTMENT OF PHYSICAL CHEMISTRY, INSTITUTE OF CHEMISTRY, FACULTY OF SCIENCE, P.J. ŠAFÁRIK UNIVERSITY, MOYZESOVA 11, SK-041 54 KOŠICE, SLOVAK REPUBLIC
**** INSTITUTE OF EXPERIMENTAL PHYSICS, SLOVAK ACADEMY OF SCIENCES, WATSONOVA 47, SK-040 01 KOŠICE, SLOVAK REPUBLIC
♯   Corresponding author: sulek@agh.edu.pl

Hermawan at al. prepared alloys containing from 20 to 35 wt.% manganese by blending, compaction and sintering from elemental Fe and Mn powders. After several rolling-resintering cycles, the samples possessed an austenite structure and exhibited mechanical properties comparable to those of 316L stainless steel [4, 5]. The corrosion rates of samples in a modified Hank's solution were determined by the use of an immersion method. The corrosion rate of the material Fe-25wt.%Mn was 0.52 mm year^{-1}, which is slightly higher than the rate 0.44 mm year^{-1} found for Fe-35wt.%Mn. This could be related to differences in microstructure. In the Fe-25wt.%Mn sample, the ε-martenzite and γ-austenite phases coexist and serve as micro-galvanic sites accelerating corrosion, while the Fe-35wt.% Mn has only γ-austenite phase. The degradation rates of both materials were higher than those of pure iron (0.22-0.24 mm year^{-1}) [6].

Nevertheless, degradation rates of Fe-Mn alloys may still be considered too low for practical applications. In that context, new biodegradable alloys were developed by adding another elements, e.g. Fe-Mn-Pd [7], Fe-Mn-C-Pd [8].

In the above mentioned binary Fe-Mn systems, the iron and manganese were uniformly distributed within the material. In the contribution presented here we report on the results of an attempt to accelerate the degradation of Fe-Mn systems by creation of microgradients in concentration of elements in the sample. Due to the variation in chemical composition on small scales, each grain can be considered as composed of „different metals" in mutual contact, which after immersion into electrolyte creates many additional micro-galvanic cells initiating and accelerating corrosion in comparison with a homogeneous sample.

2. Experimental

Pure Fe samples and samples from Fe-Mn alloys were prepared from elemental iron and manganese powders. We used water-atomized iron powder, Höganäs, ASC 100.29 grade, and manganese powder, fraction <45 μm. Powders were mixed in a turbula mixer for 20 minutes. The mixtures with 25 wt.% Mn and 30 wt.% Mn were prepared. The powder mixtures were cold pressed in a cylindrical die at 600 MPa (Φ10x10mm^3) without lubricant.

The compacts were isothermally sintered in a laboratory tube furnace ANETA at the temperature of 1120°C for 60 min and cooled to the room temperature. The heating and cooling rate was kept at 10°C/min. The gas mixture of 10% H$_2$ – 90% N$_2$ (purity of 5.0) was used as a sintering atmosphere. The flow-rate of the processing atmosphere was 4 l/min. Atmosphere drying was performed utilizing zeolite molecular sieve dryers. The inlet dew point (monitored by the SHAW Super-Dew Hygrolog) was about -59°C. Compact density values before and after sintering were obtained by weighing and measuring the dimensions of compacts.

Specimens selected for metallographic analysis were polished with 0.1 μm diamond paste and etched in 2% nital solution. The microstructure of specimens was investigated using optical microscope (OLYMPUS GX71, Japan) and scanning electron microscope coupled with the energy dispersive spectrometer (JEOL JSM-7000F, Japan with EDX INCA).

The Vickers microhardness (HV 0.01) of samples has been investigated using a micro hardness tester LECO LM-700AT. For each sample, 200 indents were performed.

Corrosion properties were investigated using a potentiodynamic polarization method by the use of the Autolab Potentiostat PGSTAT 302N. Measurements were carried out with a conventional three-electrode arrangement with the Ag/AgCl reference electrode, platinum counter electrode and iron or iron-manganese sample as the working electrode. The Hank's solution, composed of 8.00 NaCl, 1.00 Glucose, 0.60 KH$_2$PO$_4$, 0.40 KCl, 0.35 NaHCO$_3$, 0.14 CaCl$_2$, 0.10 MgCl$_2$ 6H$_2$O, 0.06 MgSO$_4$ 7H$_2$O, and 0.06 NaH$_2$PO$_4$ 2H$_2$O (in g/l) with a pH value of 7.4, was used as an electrolyte. In all experiments, the temperature was maintained at 37°C±1°C. Before the polarization tests, the samples were kept immersed in the electrolyte for 1 hour and the evolution of the open-circuit potential (OCP) was recorded. Polarization curves were obtained by varying the applied potential from -800 mV up to -200 mV at the scan rate of 0.1 mV/s. Corrosion current, corrosion potential and corrosion rate were determined by the use of the Tafel extrapolation method.

3. Overall dimensional changes of cylindrical samples

Upon sintering at 1120°C, the compacts from pure Fe powders shrank in every direction and compacts from mixed Fe and Mn powders swelled in every direction (Tab. 1). The compacts from Fe powders shrank only slightly in diameter but markedly in height (in the direction parallel to the compaction direction). For compacts from Fe-Mn mixtures, the relative elongation of height was nearly the same as that of diameter.

TABLE 1

Density and dimensional changes of compacts from the tested materials

Material	Change of height $\Delta h/h$ [%]	Change of diameter $\Delta\Phi/\Phi$ [%]	Density after sintering [g/cm^3]	Total porosity [%]
Fe	−0.176	−0.008	6.69	14.5
Fe-25wt.%Mn	+4.700	+4.623	5.54	28.7
Fe-30wt.%Mn	+5.154	+5.070	5.41	29.9

During sintering, Mn is transported through the gas phase to the Fe surfaces. Subsequently, Mn diffuses in Fe matrix and forms a solid solution with Fe, expanding thus the Fe particles. Pores remain on the sites of the Mn carrier particles, and as the sample cools, they are filled with agglomerates of tiny Mn particles. The consequence of these processes is a macroscopic expansion [9].

4. Microstructure

After sintering lasted for 60 minutes at 1120°C, previously ferritic iron particles are austenite-rimmed while their cores are still fully ferritic. Between austenitic rims and ferritic core, there is an area with a fine-grain structure (Fig. 1). The

concentration of Mn increases from the grain core towards its boundary. The EDX analysis also revealed the presence of oxygen. This should be a consequence of a high affinity of manganese to oxygen, which implies the possibility of considerable oxidation during sample processing even when a high purity sintering atmosphere is applied [10].

Free manganese is observed on the particle's boundary (Fig. 1). Residues of manganese particles have a form of agglomerate and, according to the results of SEM+EDX analyses, they are formed by manganese, manganese oxide with small amount of manganese sulphide.
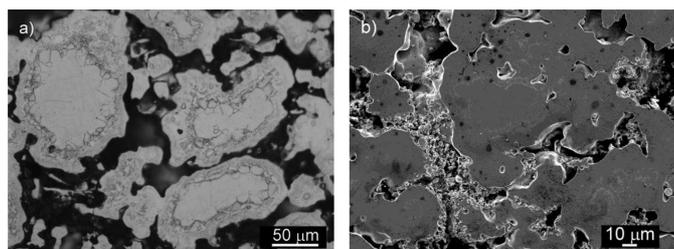

Fig. 1. Microstructure of Fe-30wt.%Mn material after sintering at 1120°C for 60 min (a) LM micrograph of sample etched by nital, (b) SEM micrograph

5. Microhardness

The Vickers microhardness at various points of samples has been investigated using a micro hardness tester LECO LM-700AT with indentation loadings of 10 G (0.1N). For each sample, 200 indents were performed. Microhardness measurements made at different points of the specimen enabled us to study the distribution of hardness values throughout the sample and to determine the range for these values, which reflects the character of microstructure of the examined material.

For the samples from a pure iron, the range (interval) of observed microhardness values is narrow and the frequency of occurrence reveals a clear peak for the hardness value of 146 MPa (Fig. 2). This is a consequence of relatively uniform microstructure of samples. For samples from a mixture containing 25wt.%Mn, the range of observed microhardness values spreads to the region of higher values, inaccessible for a pure iron, and the frequency of occurrence becomes flatter without clear peak (Fig. 2). This is a consequence of the creation of a quasicontinuous microgradient structure, with concentration of Mn increasing from the core of iron grain towards to its periphery, and strengthening of the material due to formation of solid solution and precipitation of Mn within Fe matrix. For samples from a mixture containing 30wt.% Mn, the range of observed microhardness values is similar as for samples Fe-25wt.%Mn, but there is clearly most frequently occurring value of about 340 MPa (Fig. 2). This is caused by the fact that in addition to the strengthening of ferrite due to solid solution and precipitation by Mn, the samples are also affected by creation of austenite, by a fine-grain structure between austenitic rims and ferritic core and porosity. For Fe-30wt.%Mn, the larger volume of iron grain is notably alloyed with Mn. Characteristics of the distribution of hardness values are summarized in Tab. 2.
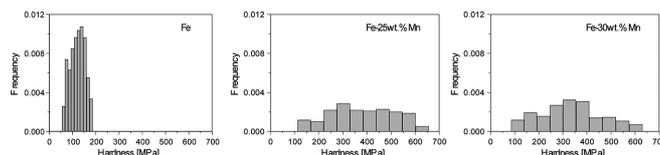

Fig. 2. The relative frequency density as a function of values of microhardness HV 0.01 for sintered samples from pure iron, Fe-25wt.%Mn and Fe-30wt.%Mn

TABLE 2

Characteristics of the distribution of hardness values

	Fe	Fe-25wt.%Mn	Fe-30wt.%Mn
arithmetic average of measured hardness values [MPa]	123.33	382.43	336.79
standart deviation [MPa]	32.67	134.28	133.48

6. Electrochemical corrosion behaviour

Figure 2 presents the time evolution of the open-circuit potential (OCP) of Fe, Fe-25wt.%Mn and Fe-30wt.%Mn electrodes immersed in the Hank's solution. For these three materials, the electrode from Fe possessed the highest open-circuit potential, and the potential of the electrode from Fe-25wt.%Mn was the lowest one. A continuous reduction of potential of Fe electrode in Hank's solution was observed during the test. The passive layer on sample surface, which to some extent protected the iron material, is dissolved during the test, so the iron showed an increasing tendency to corrode.

For the Fe electrode, a series of spikes was observed on the open-circuit potential as a function of time record. It was reported by Cheng et al. [11, 12] that the corrosion of Fe in Hank's solution is the localized one. Generally, pits were easily formed in the corroding pure iron due to localized acidification beneath the hydroxide layer, where the surface material was lost and small micro-pores were created. This random events can generate the spikes observed on the OCP vs. time curve. For Fe-Mn system, with a second phase uniformly distributed in the iron matrix, widespread galvanic corrosion took place with multiple very tiny pits formed and hydroxide products uniformly covering the surfaces, resulting in general macroscopically uniform corrosion of the material. The open-circuit potential is therefore a smoother function of time.
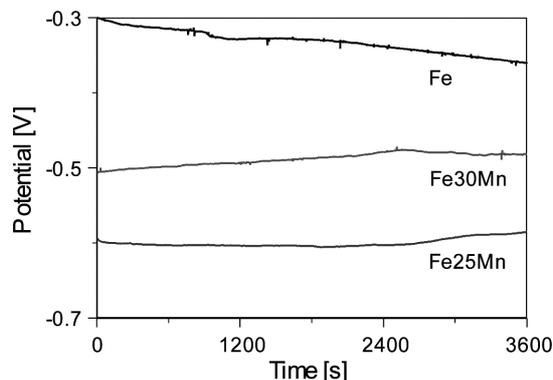

Fig. 3. The time evolution of the open-circuit potential of Fe, Fe-25wt.%Mn, Fe-30wt.%Mn electrodes immersed in Hank's solution

642

The surface layer of corrosion products consists of a red-brownish hydroxide layer followed by a black-grayish oxide layer.

Degradation rates of iron and Fe-Mn alloys immersed in the Hank's solution were examined by polarisation method at 37°C. The reproducibility of Tafel plots was good. The corrosion potential (E_{corr}) and corrosion current (i_{corr}) were calculated from the intersection of the anodic and cathodic Tafel lines extrapolations. All values of E_{corr} and i_{corr} are summarized in Tab. 3. The addition of manganese resulted in lower (less noble) corrosion potentials. This negative shift indicates the increased corrosion susceptibility of iron samples containing manganese (Fig. 3).
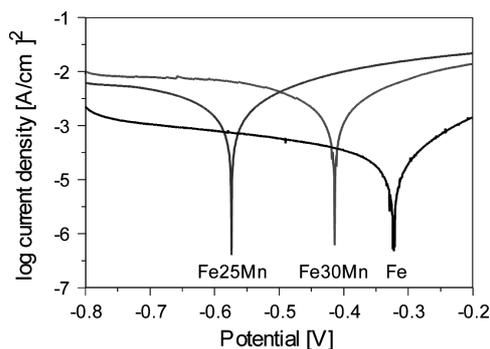

Fig. 4. Polarisation curves for iron and iron manganese samples in Hank's solution at 37°C; semilogarithmic form

TABLE 3

The values of E_{corr}, i_{corr} and corrosion rates obtained for Fe, Fe-25wt.%Mn and Fe-30wt.%Mn specimens immersed in Hank's solution

Sample	E_{corr} [mV]	i_{corr} [A/m^2]	Corrosion rate [mm/year]
Fe	−322	0.10	0.14
Fe-25wt.%Mn	−574	1.03	1.71
Fe-30wt.%Mn	−412	1.07	1.79

The corrosion current density (i_{corr}) of Fe sample was approximately ten times lower than i_{corr} of Fe-25wt.%Mn sample and Fe-30wt.%Mn sample. The difference in corrosion current densities between Fe-25wt.%Mn and Fe-30wt.%Mn samples was not significant and the corrosion rates calculated from corrosion current densities were of the same order of magnitude. Thus the corrosion resistance of Fe samples was much higher than that of the Fe-Mn samples.

The corrosion rates of porous samples are higher than the ones reported for nonporous iron based samples. This could be assigned to the higher surface area, roughness, and penetrable structure of material.

7. Conclusions

The iron and iron-manganese samples were prepared by a powder metallurgical route. It was investigated how the addition of 25 wt.%Mn and 30wt.%Mn to the iron powder affects dimensional changes, microstructure, microhardness and

in vitro electrochemical degradation of prepared sintered samples.

Upon sintering, the compacts from Fe powders contracted and samples from iron and manganese powders notably swelled. The larger the content of Mn, the larger was the swelling.

The increase of microhardness of some regions of the sample due to the presence of manganese was observed. The highest values of microhardness were detected for some regions of Fe-25wt.%Mn sample. The further increase of Mn amount (Fe-30wt.%Mn) caused the lowering of microhardness values.

When immersed in the Hank's solution, the corrosion potential of a pure iron sample decreased with time, with sudden spikes occurring from time to time, while the corrosion potential of Fe-Mn samples was nearly constant smooth function of time. This indicated the localised corrosion for pure iron sample and more uniform corrosion of Fe-Mn sample.

It was found that the addition of 25 and 30wt.%Mn resulted in a negative shift of the corrosion potential in Hank's solution. Based on the electrochemical data, it was found that the corrosion rate decreases from Fe-30wt.%Mn, through Fe-25wt.%Mn to Fe. Porous structure of sintered iron alowed increase in degradation rate.

The iron based alloys prepared by a powder metallurgical route seem to be promising candidates for degradable biomaterials. Nevertheless, further work on the regulation of the biocorrosion rate, on the improvement in mechanical properties and on the reduction of the cytotoxicity has to be done.

REFERENCES

[1] Y. Yun, et al., Materials Today **12**, 22 (2009).
[2] M. Peuster, C. Hesse, T. Schloo, C. Fink, P. Beerbaum, C. von Schnakenburg, Biomaterials **27**, 4955 (2006).
[3] R. Waksman, R. Pakala, R. Baffour, R. Seabron, D. Hellinga, F.O. Tio, J. Interv. Cardiol **21**, 15 (2008).
[4] H. Hermawan, D. Dubé, D. Mantovani, Acta Mater **6**, 1693 (2009).
[5] H. Hermawan, D. Dubé, D. Mantovani, Journal of Biomedical Materials Research Part A **93**, 1, 1 (2010).
[6] H. Hermawan, A. Purnama, D. Dube, J. Couet, D. Mantovani, Acta Biomateria **6**, 1852 (2010).
[7] F. Moszner, A.S. Sologubenko, M. Schinhammer, RC. Lerchbacher, A.C. Hänzi, H. Leitner, P.J. Uggowitzer, J.F. Löffler, Acta Materialia **59**, 981 (2011).
[8] M. Schinhammer, CM. Pecnik, F. Rechberger, A.C. Hänzi, J.F. Löffler, P.J. Uggowitzer, Acta Materialia **60**, 6-7, 2746 (2012).
[9] H. Danninger, C. Gierl, Science of Sintering **40**, 33 (2008).
[10] E. Hryha, E. Dudrová, L. Nyborg, Metallurgical and Materials Transactions A : Physical Metallurgy and Materials Science **41**, 2880 (2010).
[11] J. Cheng, Y.F. Zheng, J. Biomed. Mater. Res. B: Appl. Biomater. **101B**, 485 (2013).
[12] J. Cheng, B. Liu, Y.H. Wu, Y.F. Zheng, J. Mater. Sci. Technol. **29**, 619 (2013).